

# Automated numerical characterization of dilute semiconductors per comparison with luminescence

X. Yang<sup>1</sup> · C. I. Oriaku<sup>2</sup> · J. P. Zubelli<sup>1</sup> · M. F. Pereira<sup>3</sup> 

Received: 26 December 2016 / Accepted: 20 January 2017 / Published online: 8 February 2017  
© The Author(s) 2017. This article is published with open access at Springerlink.com

**Abstract** This paper combines analytical approximations for the optical absorption and luminescence of semiconductors with trust region-reflective methods, delivering a robust numerical characterization method to be used in the study of new bulk semiconductors per direct comparison with experimental spectra. It further extends recent applications of the theory to the case of dilute nitride semiconductors and confirms results for the s-shape of the luminescence peak as a function of temperature.

**Keywords** Semiconductors · Dilute nitrides · Luminescence · Mid infrared · Many body effects

## 1 Introduction

The study of new semiconductor materials is important from a fundamental science point of view and for the ever increasing number of applications in optoelectronics. Concrete progress requires accurate and simple modelling that can predict optical properties and become a tool for numerical characterization and device design from the ultra-violet to the

---

This article is part of the TopicalCollection on TERA-MIR: Materials, Generation, Detection and Applications (SMMO 2016).

---

Guest Edited by Mauro Pereira, AnnaWójcik-Jedlinska, Trevor Benson, Marian Marciniak, Filipa Prudencio and Marco Ribeiro.

---

✉ M. F. Pereira  
m.pereira@shu.ac.uk

<sup>1</sup> Instituto de Matematica Pura e Aplicada, Rio de Janeiro 22460-320, Brazil

<sup>2</sup> Department of Physics, Michael Okpara University of Agriculture, P.M.B. 7267, Umudike, Nigeria

<sup>3</sup> Materials and Engineering Research Institute, Sheffield Hallam University, Sheffield S1 1WB, UK

THz range and Mid Infrared Ranges (Jepsen et al. 2013; Gu et al. 2014; Krier et al. 2012; De la Mare et al. 2009; Zhuang et al. 2008). Furthermore, understanding the properties of new bulk semiconductors has attracted renewed interest in the solar cell material arena to avoid environmentally unfriendly materials such as Cd (Vidal et al. 2010).

The importance of the Coulomb interaction leading to many body and correlation effects is now a well-established fact from bulk to quantum dots and the associated non-linear effects become significantly pronounced when a semiconductor is highly excited with light fields or electrically injected carriers (Chemla and Shah 2001). Strong light fields create electron–hole pairs, which in turn constitute quantum mechanical many body systems interacting in various ways, e.g. band gap renormalization, band filling and Coulomb enhancement, screening and dephasing arising from the attractive and repulsive scattering processes from electrons, holes, phonons and impurity defects. At low temperatures and small carrier densities, excitonic effects dominate the optical absorption of bulk semiconductors and the excitons are bleached as the temperature and excitation densities increase due to a combination of screening, band filling and dephasing effects. But even at higher temperatures and densities, the Coulomb interaction is important (Chemla and Shah 2001) and plasma theories have delivered excellent approximations for the absorption and gain in this case and have been successfully applied to different isotropic bulk materials (Banyai and Koch 1986) and superlattices treated as effective anisotropic media (Pereira 1995, 2016). Photoluminescence is crucial to characterise new materials and devices under development and this paper combines analytical approximations for the optical absorption and luminescence of semiconductors with Trust Region-Reflective (TRR) methods, delivering a robust numerical characterization method to be used in the characterisation of new bulk semiconductors per direct comparison with experimental spectra. It further extends recent applications of the theory (Oriaku and Pereira 2017) to the case of dilute nitride semiconductors and confirms results for the s-shape of the luminescence peak as a function of temperature.

## 2 Mathematical formalism

An interesting feature of dilute semiconductor material is the anomalous energy emission peaks at low temperatures, following an unusual s-shape behaviour that is associated with disorder and localization effects, which have been seen in both dilute bismides (Mazzucato et al. 2014) and nitrides (Krier et al. 2012). A simple and efficient method to describe this and other light emission effects in those materials is used here (Oriaku and Pereira 2017), based on analytical solutions for the Photon Green's functions approach (Pereira and Henneberger 1996, 1998; Michler et al. 1998), delivering a microscopic, fully quantum mechanical solution. Note that, in spite of its success to accurately explain experiments such as both single beam and nonlinear pump-probe photoluminescence (Michler et al. 1998), as well as being a powerful tool to design optical devices and solar cells (Aeberhard 2011).

Nonequilibrium Green's Functions (NEGF) techniques that include Photon Green's functions mentioned above and semiconductor Bloch equations, can be applied to both intersubband (Pereira 2011, 2016; Pereira and Faragai 2014) and interband transitions (Pereira et al. 1994; Grempel et al. 1996), but usually requires intensive numerical methods. Therefore, in this project, we did not fully calculate the dephasing attributed to electron–phonon, electron-impurity and electron-alloy disorder scattering and that leads to

measured s-shape-like features in dilute semiconductor samples (Imhof et al. 2010; Kesaria et al. 2015). The scattering processes cited above can all be described by selfenergies (Pereira 1995; Wacker 2002; Schmielau and Pereira 2009). Instead, we used Trust Region-Reflective (TRR) methods (Hung 2012) to obtain the values of carrier density, homogeneous and inhomogeneous broadening that best characterize experimental results and as a future step, we shall use these numbers to compare and contrast with Nonequilibrium Green's Functions (NEGF) calculations to help determine the relative influence of each scattering/dephasing mechanisms.

The quantum mechanical Poynting vector describing light emission can be expressed in terms of the Photon Green's Function, leading to the optical power density spectrum, which can be directly compared with photoluminescence experiments (Oriaku and Pereira 2017).

$$I(\omega) = \frac{I_0}{1 + \exp(\beta(\hbar\omega - \mu))} \left\{ \sum_{n=1}^{\sqrt{g}} \frac{4\pi}{n} \left( \frac{1}{n^2} - \frac{n^2}{g^2} \right) \delta_{\Gamma}(\zeta - e_n) + 2\pi \int_0^{\infty} \frac{\sinh(\pi g \sqrt{x})}{\cosh(\pi g \sqrt{x}) - \cos(\sqrt{4g - g^2 x})} \delta_{\Gamma}(\zeta - x) dx \right\}, \quad (1)$$

where  $I_0 = \frac{\hbar\omega^2 e^2 |\Pi|^2}{\pi e_0 c^3 a_0^3}$ ,  $e_{n=-(n^{-1}-ng^{-1})^2}$ ,  $\zeta = (\hbar\omega - E_g)/e_0$ ,  $g = (\kappa a_0)^{-1}$  and  $a_0, e_0$  denote, respectively the exciton Bohr radius and binding energy.

Fluctuations in the alloy composition are described here by a Gaussian distribution in the dilute Bi mole fraction  $x$ . If  $x_0$  is the nominal Bi mole fraction, and  $I(x, \omega)$  is the expression in Eq. 8, the inhomogeneously broadened spectrum reads

$$I_{inh}(\omega) = \frac{1}{\sqrt{2\pi}\sigma} \int_{x_0-3\sigma}^{x_0+3\sigma} I(x, \omega) e^{-\left(\frac{x-x_0}{\sigma}\right)^2} dx \quad (2)$$

Thus, in order to compare our calculations with experimental data, we need three main parameters: the carrier density, the inhomogeneous broadening parameter and the homogeneous dephasing:  $(\rho, \sigma, \Gamma)$ .

### 3 Numerical method and results

In our model,  $u_T(\rho, \sigma, \Gamma)$  is the luminescence peak energy function at temperature  $T$ . In the cases that we have investigated, the carrier density, inhomogeneous and homogeneous broadening are restricted to the following intervals (normalized units are used here)  $\in [1.5 \times 10^{14}, 10^{17}]$ ,  $\sigma \in [10^{-3}, 2.5 \times 10^{-3}]$  and  $\Gamma \in [1, 2]$ .

Experimental data such as in Refs. Krier et al. (2012) and Mazzucato et al. (2014) provides the luminescence peak energy at different temperatures for InAsN. Thus, by applying the least squares method, we can estimate the parameters  $(\rho, \sigma, \Gamma)$  so that the residual between the theoretical function and the experimental data is minimized. Since the scales of the parameters are different by several orders of magnitude, we introduce auxiliary variables,  $\hat{\rho} = \log(\rho)$ ,  $\hat{\sigma} = 10^4 \sigma$ ,  $\hat{\Gamma} = 10\Gamma$ . That leads to a transformed function,  $u_T(\rho, \sigma, \Gamma) = \hat{u}_T(\hat{\rho}, \hat{\sigma}, \hat{\Gamma})$ . Krier et al. (2012) provides a series of data points  $d = (d_1, d_2, \dots, d_N)$  measured at  $T = (T_1, \dots, T_N)$ . Therefore, the problem becomes:

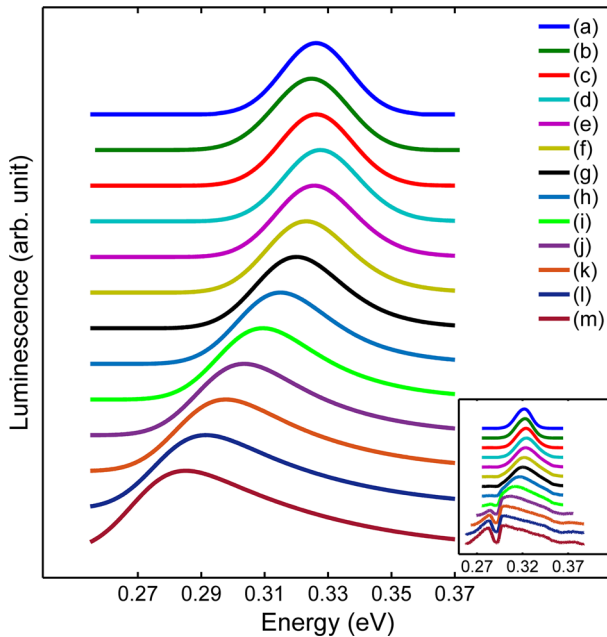


**Fig. 1** Theoretical versus experimental (*inset*) luminescence for a InAsN sample at various temperatures. From *a* to *m* the temperatures are: 4, 20, 40, 60, 80, 100, 120, 150, 180, 210, 240, 270 and 300 K. The low energy feature (around 0.28 meV) at high temperatures is due to the presence of CO<sub>2</sub> in the optical path of the measurements. The experimental data for comparison has been extracted from Krier et al. (2012). The density used in the calculations is  $N = 10^{14}$  carriers/cm<sup>3</sup>

$$\min_{x=(\rho,\sigma,\Gamma)} \sum_{i=1}^N (\dot{u}_{t_i} - d_i)^2. \quad (3)$$

In order to address this problem, we selected the function `lsqnonlin` in Matlab, which applies Trust Rion-Reflective (TRR) methods. Compared with other techniques, such as line-searching methods, TRR delivers more accurate and less time costly results. In a nutshell, the reasoning underlying the TRR approach is as follows: Suppose we wish to minimize  $F(x)$ . In order to find a point  $x_{i+1}$  with a smaller function value, we proceed by minimizing the following quadratic model:

$$\min_{s \in N} m(s) = g^T s + \frac{1}{2} s^T H s, \quad (4)$$

where  $N$  is a neighbourhood of  $x_i$  and is called the trust region.  $g$  and  $H$  are the gradient and Hessian of  $F$ . particular,  $s \in N$  is equivalent to  $\|D_i s\| < \Delta_i$ , where  $D_i$  is a diagonal scaling matrix and  $\Delta_i$  is a positive scalar. Then the current point is updated to  $x_i + s$  if  $F(x_i + s) < F(x_i)$ ; otherwise, the current point remains unchanged, ( $x_{i+1} = x_i$ ), the region of trust is shrunk and the trial step computation is repeated. In other words, we set the new step size  $\Delta_{i+1} \in (0, \tau \Delta_i]$ , given a scaling factor  $0 < \tau < 1$ .

In order to solve for  $s$  in Eq. (4), there are several good algorithms. However, they require time proportional to several factorisations of  $H$ . Therefore, for trust-region problems, a more efficient approach is needed. The approximation approach followed in

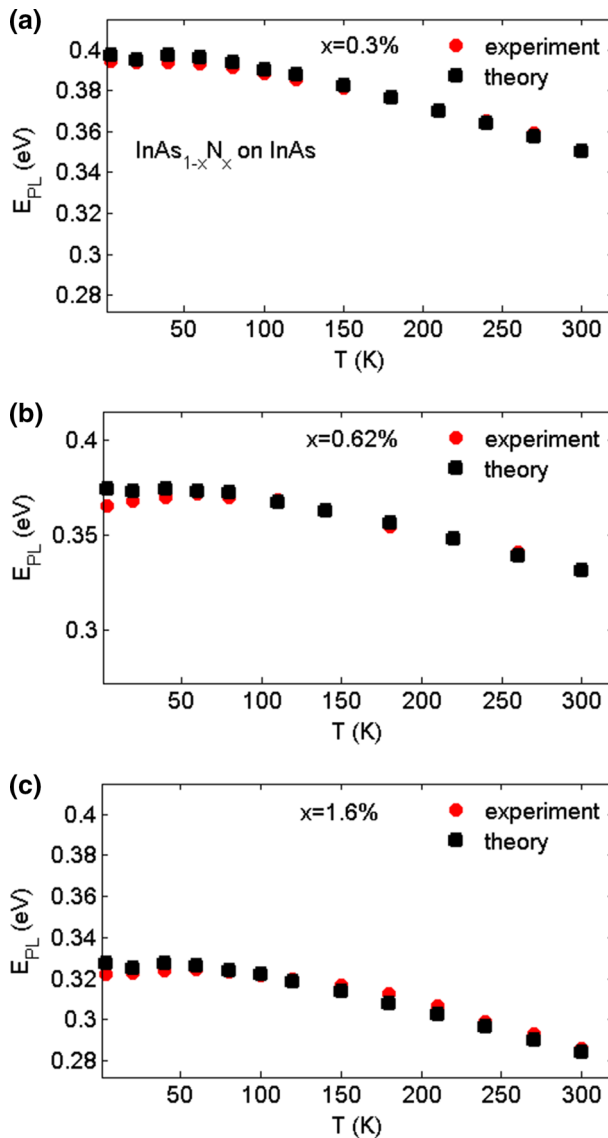


**Fig. 2** Plot of peak PL energy  $E_{PL}$  (eV) versus  $T$  (K) for the mole fractions **a**  $x = 0.3\%$ , **b**  $x = 0.62\%$ , **c**  $x = 1.6\%$  of InAs<sub>1-x</sub>N<sub>x</sub> on InAs. Good agreement can be observed between the theory (black) and experiments from Krier et al. (2012). The carrier density used is  $n = 10^{15} \text{ cm}^{-3}$

Optimization Toolbox solvers is to restrict the trust-region subproblem to a two-dimensional subspace  $S$  (Branch et al. 1999; Byrd et al. 1988). Once the subspace  $S$  has been computed, the work to solve Eq. (4) is trivial even if full eigenvalue/eigenvector information is needed, since in the subspace, the problem is only two-dimensional. The dominant work has now been shifted to the determination of the subspace.

The two-dimensional subspace  $S$  is determined with the aid of a pre-condition conjugate gradient described below. The solver defines  $S$  as the linear space spanned by  $s_1$  and  $s_2$ ,

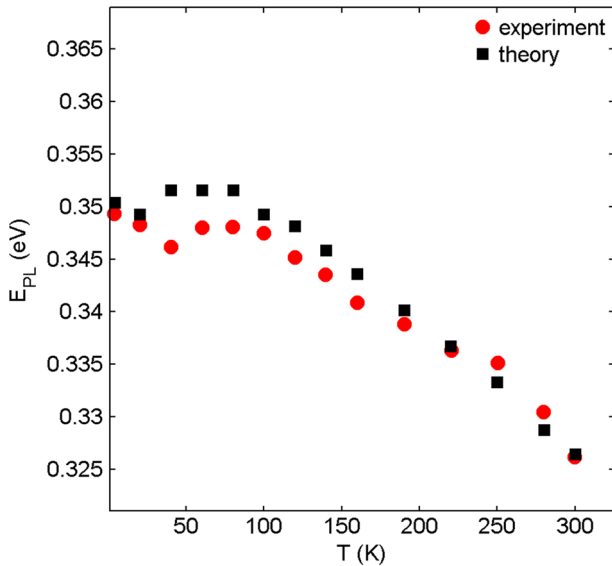


**Fig. 3** Plot of peak PL energy  $E_{PL}$  (eV) versus  $T$  (K) for  $\text{InAs}_{1-x}\text{Nx}$  on GaAs. The experimental data has been extracted from Krier et al. (2012). Good agreement can be observed between the theory (black) and experiments from Krier et al. (2012). The carrier density used is  $n = 10^{15} \text{ cm}^{-3}$

where  $s_1$  is the direction of the gradient  $g$  and  $s_2$  is either an approximate Newton direction, i.e., a solution to

$$H \cdot s_2 = -g, \quad (5)$$

or a direction of negative curvature,

$$s_2^T \cdot H \cdot s_2 < 0. \quad (6)$$

The philosophy behind this choice of  $S$  is to force global convergence (via the steepest descent directive or negative curvature direction) and achieve fast local convergence (via the Newton step, when it exists).

In our Numerical Experiments for Ref. Mazzucato et al. (2014), confirming the results found in Ref. Oriaku and Pereira (2017), the initial values for  $(\rho, \sigma, \Gamma)$  were  $[1E15, 2E-3, 1]$ . After nine iterations, the trust region shrank and the optimal values remained the same with the initial. These initial values were obtained by try and error during several runs. Therefore, we conclude that the local minimum for the function is found.

Figures 1 and 2 show results of the comparison between theory and experiments in Ref. Krier et al. (2012), extending the findings of Ref. Oriaku and Pereira (2017) for the InAsN case.

It is interesting to see that lower quality interfaces lead to more scattering and thus to a more pronounced s-shape as shown in Fig. 3 where InAsN is grown on GaAs.

In summary, the automated numerical method developed validated our previous work that took days of trial and error attempt for a single data set. It can now be applied to a number of new materials, serve as guideline to interpret experimental data and to guide the choice of microscopic models that better deliver agreement with experiments. The

comparison with experiments for the InAsN nitride case further validates our method as a powerful tool to support the characterization and development of new materials and devices.

**Acknowledgements** The authors acknowledge support from COST ACTION MP1204, TERA-MIR Radiation: Materials, Generation, Detection and Applications.

**Open Access** This article is distributed under the terms of the Creative Commons Attribution 4.0 International License (<http://creativecommons.org/licenses/by/4.0/>), which permits unrestricted use, distribution, and reproduction in any medium, provided you give appropriate credit to the original author(s) and the source, provide a link to the Creative Commons license, and indicate if changes were made.

## References

- Aeberhard, U.: Theory and simulation of quantum photovoltaic devices based on the non-equilibrium Green's function formalism. *J. Comput. Electron.* **10**(4), 394–413 (2011)
- Banyai, L., Koch, S.W.: A simple theory for the effects of plasma screening on the optical-spectra of highly excited semiconductors. *Z. Phys. B* **63**(3), 283–291 (1986)
- Branch, M.A., Coleman, T.F., Li, Y.: A sub-space, interior, and conjugate gradient method for large-scale bound- constrained minimization problems. *SIAM J. Sci. Comput.* **21**(1), 1–23 (1999)
- Byrd, R.H., Schnabel, R.B., Shultz, G.A.: Approximate solution of the trust region problem by minimization over two-dimensional subspaces. *Math. Program.* **40**(1–3), 247–263 (1988)
- Chemla, D.S., Shah, J.: Many-body and correlation effects in semiconductors. *Nature* **411**(6837), 549–557 (2001)
- De la Mare, M., Zhuang, Q., Krier, A., Patanè, A., Dhar, S.: Growth and characterization of InAsN/GaAs dilute nitride semiconductor alloys for the midinfrared spectral range. *Appl. Phys. Lett.* **93**(3), 031110 (2009)
- Grempe, H., Diessel, A., Ebeling, W., Gutowski, J., Schüll, K., Jobst, B., Hommel, D., Pereira, M.F., Henneberger, K.: High-density effects, stimulated emission, and electrooptical properties of ZnCdSe/ZnSe single quantum wells and laser diodes. *Phys. Status Solidi* **194**(1), 199–217 (1996)
- Gu, Y., Wang, K., Zhou, H., Li, Y., Cao, C., Zhang, L., Zhang, Y., Gong, Q., Wang, S.: Structural and optical characterizations of InPBi thin films grown by molecular beam epitaxy. *Nanoscale Res. Lett.* **9**(1), 24 (2014)
- Hung, J.: Energy Optimization of a Diatomic System. University of Washington, Seattle, WA. <http://www.math.washington.edu/~morrow/papers/jane-thesis.pdf> (2012)
- Imhof, S., Thränhardt, A., Chernikov, A., Koch, M., Köster, N.S., Kolata, K., Chatterjee, S., Koch, S.W., Lu, X., Johnson, S.R., Beaton, D.A.: Clustering effects in Ga (AsBi). *Appl. Phys. Lett.* **96**(13), 131115 (2010)
- Jepsen, P.U., Cooke, D.G., Siegel, P.H.: Introduction to the special issue on terahertz spectroscopy. *IEEE Trans. Terahertz Sci. Technol.* **3**(3), 237–238 (2013)
- Kesaria, M., Birindelli, S., Velichko, A.V., Zhuang, Q.D., Patanè, A., Capizzi, M., Krier, A.: In (AsN) mid-infrared emission enhanced by rapid thermal annealing. *Infrared Phys. Technol.* **68**, 138–142 (2015)
- Krier, A., De la Mare, M., Carrington, P.J., Thompson, M., Zhuang, Q., Patanè, A., Kudrawiec, R.: Development of dilute nitride materials for mid-infrared diode lasers. *Semicond. Sci. Technol.* **27**, 4009 (2012)
- Mazzucato, S., Lehec, H., Carrère, H., Makhloufi, H., Arnoult, A., Fontaine, C., Amand, T., Marie, X.: Low-temperature photoluminescence study of exciton recombination in bulk GaAsBi. *Nanoscale Res. Lett.* **9**(1), 1–5 (2014)
- Michler, P., Vehse, M., Gutowski, J., Behringer, M., Hommel, D., Pereira, M.F., Henneberger, K.: Influence of Coulomb correlations on gain and stimulated emission in (Zn, Cd)Se/Zn(S, Se)/(Zn, Mg)(S, Se) quantum-well lasers. *Phys. Rev. B* **58**(4), 2055–2063 (1998)
- Oriaku, C.I., Pereira, M.F.: Analytical solutions for semiconductor luminescence including Coulomb correlations with applications to dilute bismides. *J. Opt. Soc. Am. B* **34**, 321–328 (2017)
- Pereira, M.F.: Analytical solutions for the optical absorption of semiconductor superlattices. *Phys. Rev. B* **52**(3), 1978–1983 (1995)
- Pereira Jr., M.F.: Microscopic approach for intersubband-based thermophotovoltaic structures in the terahertz and mid-infrared. *JOSA B* **28**(8), 2014–2017 (2011)

- Pereira, M.F.: Anisotropy and nonlinearity in superlattices. *Opt. Quantum Electron.* **48**(6), 1–7 (2016a)
- Pereira, M.F.: The linewidth enhancement factor of intersubband lasers: from a two-level limit to gain without inversion conditions. *Appl. Phys. Lett.* **109**(22), 222102-1–222102-4 (2016b)
- Pereira, M.F., Faragai, I.A.: Coupling of THz radiation with intervalence band transitions in microcavities. *Opt. Express* **22**(3), 3439–3446 (2014)
- Pereira, M.F., Henneberger, K.: Green's functions theory for semiconductor-quantum-well laser spectra. *Phys. Rev. B* **53**(24), 16485–16496 (1996)
- Pereira, M.F., Henneberger, K.: Microscopic theory for the influence of Coulomb correlations in the light-emission properties of semiconductor quantum wells. *Phys. Rev. B* **58**(4), 2064–2076 (1998)
- Pereira, M.F., Binder, R., Koch, S.W.: Theory of nonlinear optical absorption in coupled-band quantum wells with many-body effects. *Appl. Phys. Lett.* **64**(3), 279–281 (1994)
- Schmielau, T., Pereira Jr., M.F.: Nonequilibrium many body theory for quantum transport in terahertz quantum cascade lasers. *Appl. Phys. Lett.* **95**(23), 231111-1–231111-14 (2009)
- Vidal, J., Botti, S., Olsson, P., Guillemales, J.F., Reining, L.: Strong interplay between structure and electronic properties in CuIn(S, Se)(2): a first-principles study. *Phys. Rev. Lett.* **104**(5), 056401 (2010)
- Wacker, A.: Semiconductor superlattices: a model system for nonlinear transport. *Phys. Rep.* **357**(1), 1–111 (2002)
- Zhuang, Q., Godenir, Q., Krier, A., Tsai, G., Lin, H.H.: Molecular beam epitaxial growth of InAsN: Sb for midinfrared optoelectronics. *Appl. Phys. Lett.* **93**(12), 121903 (2008)